Design and Analysis of 2MW Horizontal Axis Wind Turbine Blade

Gizachew Dereje[1,*] and Belete Sirahbizu (Ph.D.)[2]

[1]*Mechanical Engineering, university of Gondar Institute of Technology School of mechanical Engineering*

Gondar, Ethiopia.

E-mail:anasamu120@gmail.com

[2]***Mechanical Engineering,*** Assistant Professor

College of Electrical and Mechanical Engineering University-Industry Linkage Directorate Director. Addis Ababa Science and Technology University

Addis Ababa, Ethiopia

E-mail:belete.sirhabizu@aastu.edu.et

Abstract

This paper mainly focused on the design and analysis methods that used to achieve a satisfactory level of performance of 2MW horizontal axis wind turbine blade. A design method based on blade element momentum theory is used to models and estimate the aerodynamic loads on wind turbine constructions. By applying this method a 2MW horizontal axis wind turbine rotor blade is successfully designed. A user-interface computer program is written on MATLAB 2018b to estimate the aerodynamic performance and structural analysis of the existing horizontal axis wind turbine blades. The program gives blade geometry parameters (chord and twist distributions), coefficients of performance and aerodynamic forces (trust and torque) for the following inputs; power required from the turbine, number of blades, design wind velocity and blade profile type (airfoil), maximum and minimum bending stress of the blade considering as a simple cantilever beam finally it manipulate the bending moment diagram and shear force diagrams. It also gives the three dimensional views of the designed blade elements for visualization after exported to SOLIDWORKS 2019."

Key words:

*Renewable energy, Wind turbine Blade, Aerodynamics, Blade element momentum theory,*GOE 239 (MVA H.31) air-foil.

Introduction

A wind turbine is a machine which converts the power in the wind into electricity. This is contrast to a windmill, which is a machine that converts the wind's power into mechanical power. Wind power, as an alternative to fossil fuels, is abundant, renewable, and extensively circulated, clean, produces no greenhouse gas emissions during operation and uses little land (Fthenakis *et al.*, 2002). If the efficiency of a wind turbine is increased, then more power can be generated thus decreasing the need for expensive power generation that causes pollution. Ever since the seventh century, people have been utilizing wind to make their lives easier (Satish *et al.*, 2011). Renewable energy sources are those energy sources, which are not spoiled when their energy is harnessed. Human use of renewable energy requires technologies that harness natural phenomena such as sunlight, wind, waves, water flow, and biological processes such as biological hydrogen production and geothermal heat. Amongst the above mentioned sources of energy there has been a lot of development in the technology for harnessing energy from the wind (Patnaik *et al.*, 2009). The energy transferred to the rotor by the wind depends on the air density, the swept area of the rotor and wind speed. Blade is the key component to capture wind energy. It plays a vital role in the whole wind turbine. Turbine power production depends on the interaction between the rotor and the wind (Manwell, 2002).

Wind energy in Ethiopia

Ethiopia is a country benefitting from an abundance of wind energy resources in every region. The Ethiopian government recognized the potential for harnessing this natural resource to help maintain economic growth through the energy sector and to become a major regional exporter of energy by diversifying electricity generation.

Wind energy application in Ethiopia has been limited to water pumping in the past. There is now, however, definite plan to exploit wind for power production. With the aim of diversifying the energy sources, the Ethiopian government is constructing a number of wind farms with total capacity of 1116 MW. It was mentioned that according to the growth and transformation plan adopted by the government for the period of 2011 to 2015, EEPCo has planned to build eight wind farms. Those wind farms are the 120 MW Ashegoda wind power plant in Tigre region north of the country, the 300 MW Aysha wind farm near the Djibouti border, the 100 MW Debre Birhan wind farm north of Addis Ababa, the 100 MW Assela wind power project south-east of the capital, 52 MW Adama I wind farm and the 153 MW Adama II wind power project south of the capital, the 250 MW Galema I wind power project south of the capital and the 42 MW Mesobo-Harena wind farm in Tigre region north of the country

Corporation (EEPCo), Ethiopia has a capacity of generating more than 10,000MW from wind. Considering this substantial wind resource in the country, the government has committed itself to generate power from wind plants by constructing eight wind farms with total capacities of 1,116MW. So far, two wind farms such as, Adama I and Adama II wind farms started producing 324MW and Ashegoda 120 MW. Some of the erected wind turbines in Adama I wind farm are shown in Fig.1.

Figure 1 Adama wind farm

Ashegoda wind farm is the biggest wind farm in sub Saharan Africa, consisting of 84 wind turbines including 30 Vergnet GEV HP 1MW turbines, 54 Alstom Eco 74 turbines of 1.67 MW and an GE-Grid substation connected to the national grid (230 KV/130 MVA). Some of the erected wind turbines in ashengoda wind farm are shown in Fig.2.

Figure 2Ashengoda wind farm

Problem definition

To advance turbine blade design in order to maximize the lift force on the blade and reduce drag so that the force on the blade that acts in the tangential direction is maximized, air turbine design it is crucial to reduce the trust on the turbine blades because it wastes energy and it requires a stronger blade to withstand its loading this helps to maximize annual energy production.

Wind energy conversion systems are very different in nature from conventional generators, and therefore dynamic studies must be addressed in order to integrate wind power into the power system. Wind turbines are machines that remove energy from the wind by leveraging the aerodynamic principles of lift and drag. Lift and drag forces move the turbine blades which convert kinetic wind energy to rotational energy by optimizing lift and drag principles. For this study the simulation is based on modern wind turbine design procedure; selection for best airfoil, optimum pitch angle, blade geometry in order to increase rated wind power.

Wind turbine

A wind turbine uses the aerodynamic force of the lift to rotate a shaft which in turn helps in the conversion of mechanical power to electricity by means of a generator.

Wind turbine generator which converts the kinetic energy of the wind into mechanical shaft power to drive a generator that in turn produces electrical energy. A wind turbine (WT) is composed of five main elements:

- Rotor made up of rotor blades that use aerodynamic lift to convert wind energy into mechanical energy.
- A rotor bearing fixed on a structure that causes a defined rotation of the rotor and leads to conversion of the aerodynamic wind energy into a rotational shaft torque. A yaw system maintains the horizontal rotor axis pointing upstream into the wind.
- A power conversion system that converts the low-speed rotational energy into suitable shaft power to drive an electrical generator.
- A tower and foundation structure to support the rotor and generator system at a height that harvests the most amount of energy for an acceptable capital cost.
- An electrical power distribution system that supplies the energy to the consumer in compliance with local grid code and system requirements.

For this purpose there are mainly two types of wind turbine and these are:

(a) Horizontal axis wind turbine (HAWT)
(b) Vertical axis wind turbine (VAWT)

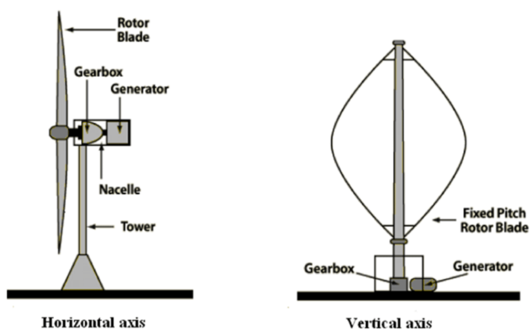

Figure 3 Horizontal and vertical wind axis turbine

Methodology and design procedure

The purpose of this project is to design a blade for a 2MW wind turbine. The first step to achieve a better power performance is the blade aerodynamic analysis. The main parameters governing the blade design of a wind. Machine includes blade diameter, blade number, and blade geometry aerofoil type and blade pitch angle.

Aerodynamic optimization of the blade is determined by the proper choice of number of blades, radial distribution of chord and twist, airfoils, tip speed ratio and pitch angle. The blades are critical components of the rotor, and consist of the airfoils which interact with the wind and convert the power in the wind to mechanical power. The design tip speed ratio of a rotor is that tip speed ratio where the power coefficient is a maximum. Selection of this value will have a major impact on the design of the wind turbine.

Blade design theory

From analysis of blade design theory, it is possible to select best airfoil for blade, so that the blade can more efficient for performance. A wind turbine rotor consists of airfoils that generate lift by virtue of the pressure difference across the airfoil, producing the same step change in pressure seen in the actuator disc type of analysis. The analysis has been done by using momentum theory and blade element theory. Momentum theory refers to a control volume analysis of the forces at the blade based on the conservation of linear and angular momentum. Blade element theory refers to an analysis of forces at a section of the blade, as a function of blade geometry. The results of these approaches can be combined into what is known as strip theory or blade element momentum (BEM) theory. This theory can be used to relate blade shape to the rotor's ability to extract power from the wind.

The blade design analysis covers the following sections,

(1) Momentum theory
(2) Blade element theory
(3) Blade-element momentum theory
(4) The Actuator Disk Theory

Blade momentum analysis

The forces on a wind turbine blade and flow conditions at the blades can be derived by considering conservation of momentum since force is the rate of change of momentum.

Blade element theory

In this theory, the blade is considered to be divided into N sections or elements as shown in figure below. It is assumed that each element is independent of the others, with no aerodynamic interaction. Also, the forces on the blades are determined only by the lift and drag characteristic of the airfoil shape of the blade. Consider a blade element at a distance 'r' from the axis. The lift and drag forces acting at an element depends on the relative velocity of air at that element

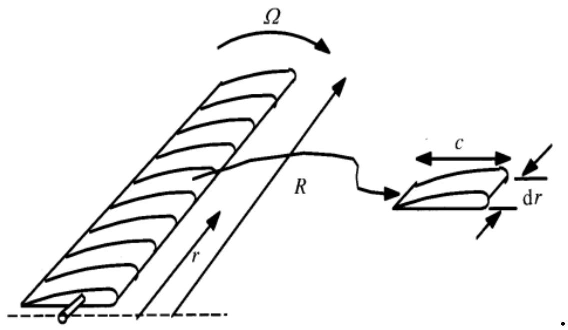

Figure 4 schematic of blade elements

Blade-element momentum theory

BEM theory refers to the determination of a wind turbine blade performance by combining the equations of general momentum theory and blade element theory by equating the elemental thrust force equations from general momentum theory and blade element theory

The momentum theory refers to a control volume analysis of the forces at the blade based on the conservation of linear and angular moment. While the blade element theory determines the forces on the blade due to the blade characteristics of lift and drag force. Both theories can be combined into what it is known as blade element momentum (BEM) theory. The BEM extends the theory of the actuator disc incorporating the influence of the rotor blades. The effect of each elemental ring is defined by analyzing the aerodynamic response of the blades to the flow in which they are immersed. The forces and moments derived from momentum theory and blade element theory must be equal. By equating, we can derive the flow conditions for a turbine design which is known as blade element momentum/strip/modified blade element theory.

Governing equations

$$\boldsymbol{dT = B\frac{1}{2}\rho U_{rel}^2(C_L\cos\varphi + C_D\sin\varphi)cdr}$$ *Equation 1*

$$\boldsymbol{dL = B\frac{1}{2}\rho U_{rel}^2(C_L\sin\varphi - C_{D\cos\varphi})cdr}$$ *Equation 2*

$$\boldsymbol{dQ = rdL}$$ *Equation 3*

$$\boldsymbol{dQ = B\frac{1}{2}\rho U_{rel}^2(C_L\sin\varphi - C_{D\cos\varphi})crdr}$$ *Equation 4*

The foremost assumption in BEM theory

- Individual stream tubes (the intersection of a stream tube and the surface swept by the blades) can be analyzed independently of the rest of the flow as assumed before for the blade element theory.
- Span wise flow is negligible, and therefore airfoil data taken from two-dimensional section tests are acceptable as assumed before in again blade element theory.
- Flow conditions do not vary in the circumferential direction, i.e.axisymmetric flow. With this assumption

the stream tube to be analyzed is a uniform annular ring centered on the axis of revolution as assumed before in general momentum theory.

The actuator disk theory

A simple model, generally attributed to Betz (1926) can be used to determine the power from an ideal turbine rotor, the thrust of the wind on the ideal rotor and the effect of the rotor operation on the local wind field. The simplest aerodynamic model of a HAWT is known as 'actuator disk model' in which the rotor becomes a homogenous disk that removes energy from the wind. Actuator disk theory is based on a linear momentum theory developed over 100 years ago to predict the performance of ship propeller.

Basic assumptions for ideal actuator disk theory

- Homogenous, Incompressible, steady state fluid flow
- No frictional drag
- The pressure increment or thrust per unit area is constant over the disk
- The rotational component of the velocity in the slipstream is zero.
- There is continuity of velocity through the disk

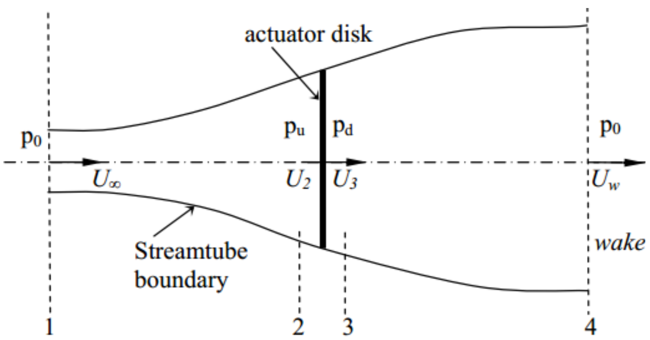

Figure 5 idealized flow through a wind turbine represented by a non-rotating actuator disk

$\boldsymbol{U_2 = U_3 = U_w}$ *Equation 5*

The turbine is represented by a uniform "actuator disk" which creates a discontinuity of pressure in the stream tube of air flowing through it. Note also that this analysis is not limited to any particular type of wind turbine

$\boldsymbol{P_0 + \frac{1}{2}\rho U_\infty^2 = P_u + \frac{1}{2}\rho U_R^2\ P_d + \frac{1}{2}\rho U_R^2}$ *Equation 6*

$$= \boldsymbol{P_0 + \frac{1}{2}\rho U_W^2}$$

$\boldsymbol{T = \dot{m}(U_\infty - U_w)}$ *Equation 7*

Vortex Theory

Vortex theory is an alternative theory which provides a method of analyzing the rotor performance. The vortex theory explains the origin of axial and angular induction factors which have been already introduced in both general momentum theory and blade element theory without giving any physical meaning about their existence. The vortex theory depends fundamentally on the conception that the lift of an airfoil section is associated with a circulation of the flow around its contour. According to modern airfoil theory the lift L per unit length of an airfoil section in two-dimensional motion is related to the circulation Γ around its contour

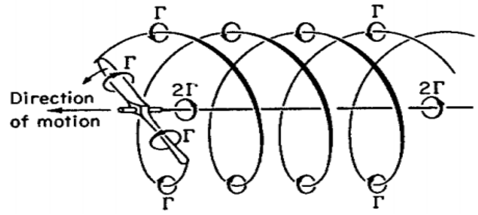

Figure 6 tip and root vortices

The results of the vortex theory:

- The induced flow at any radius r depends only on the thrust and torque grading at this radius. In other words, the blade elements at differing radii are hydro-dynamically independent. This proves the validity of the assumption about this result mentioned in blade element theory.
- The induced axial velocity at a blade element is just half the axial velocity in the distant part of the slipstream which comes from the element at that radius. This is in agreement with the findings of the actuator disk theory.
- The induced circumferential or rotational velocity of inflow at a blade element is just the half the rotational velocity in the distant part of the slipstream which comes from the elements at that radius which is what was done while defining angular induction factor in the general momentum theory.

Design Aspects

Designing a wind turbine generator essentially involves determining the turbine rating, variable or fixed speed, diameter of the rotor, number of blades, blade profile, chord length, setting angle, hub height, type of tower, transmission gears and the generator. Wind turbine manufacturers are offering various models with different rotor diameters and generator ratings so that customers can best match the distribution of wind speeds with an appropriate machine. In areas with relatively low wind speeds, a larger rotor diameter may use. In areas with relatively high wind speeds, it may be better to increase the generator rating. The impacts of grid integration such as voltage and frequency control, protection schemes, harmonic and flicker effects are also taken into consideration.

Blades

The most fundamental components of the rotor are the blades. They are the devices that convert the force of the wind into the torque needed to generate useful power

Design Considerations

There are many things to consider in designing blades, but most of them fall into one of two categories:
(1) Aerodynamic performance and
(2) Structural strength.

Underlying all of these, of course, is the need to minimize life cycle cost of energy, which means that not only should the cost of the turbine itself be kept low, but that the operation and maintenance costs should be kept low as well.

There are other important design considerations as well; they are all summarized in the following list.

- aerodynamic performance;
- structural strength;
- blade materials;
- recyclability;
- blade manufacturing;
- worker health and safety;
- noise reduction;
- condition/health monitoring;
- blade roots and hub attachment;
- passive control or smart blade options;
- Costs.

Airfoil Selection in HAWT Blade Design

The aerodynamic force can be produced by moving an aerofoil shaped body in a fluid. The lift and drag forces will characterize the blade performance. Optimal lift can be obtained as a result of angle of attack and aerofoil shape. Various standard aerofoil are available through which the blade profiles can be developed and can be characterized by their camber, thickness and chord length shown in fig. Most of this design used the concepts of BEM theory and Betz equations to determine the blade shape for standard rotors. To have maximum lift coefficient the twist distribution should be properly maintained. The aerofoil must be attributed with sound aerodynamic data that accounts for the rotation effect as it is essential to perform high fidelity CFD simulation on aerofoil

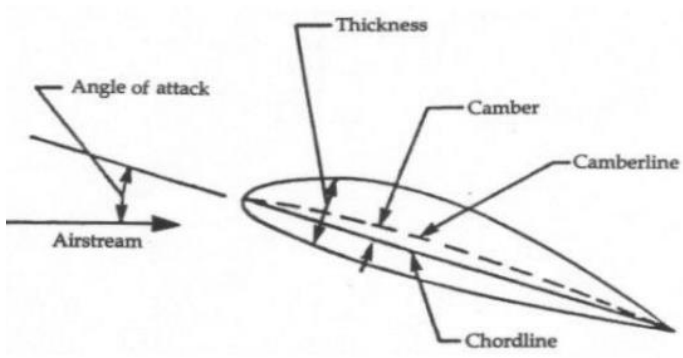

Figure 7Aero foil nomenclature

Airfoil Terminology

A number of terms are used to characterize an airfoil, as shown in Figure 8. The mean camber line is the locus of points halfway between the upper and lower surfaces of the airfoil. The most forward and rearward points of the mean camber line are on the leading and trailing edges, respectively. The straight line connecting the leading and trailing edges is the chord line of the airfoil, and the distance from the leading to the trailing edge measured along the chord line is designated the chord, c, of the airfoil. The camber is the distance between the mean camber line and the chord line, measured perpendicular to the chord line. The thickness is the distance between the upper and lower surfaces, also measured perpendicular to the chord line
Finally, the angle of attack, a, is defined as the angle between the relative wind (U_{rel}) and the chord line.

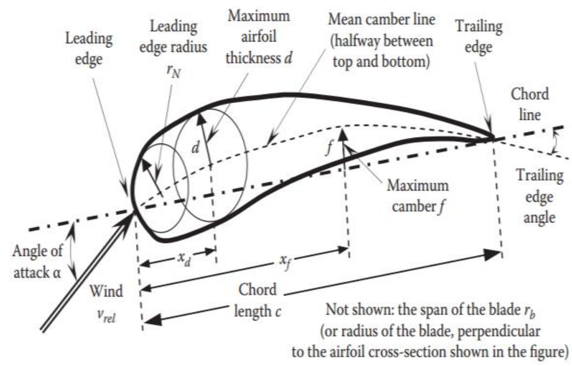

Figure 8basic description of an airfoil

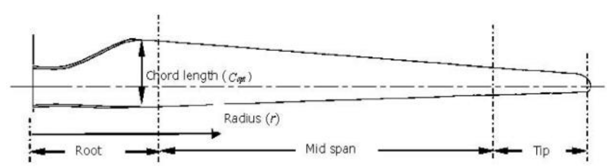

Figure 9 the three blade regions

Engineering requirements into the selection of a wind turbine airfoil

There are evidently many engineering requirements into the selection of a wind turbine airfoil. These include primary requirements related to

- aerodynamic performance,

- structural,
- strength and stiffness,
- Manufacturability and maintainability.
- The usual assumption is that high lift and low drag are desirable for an airfoil and that the drag-to-lift ratio γ which is known as glide ratio

Blade Design Procedure

Designing a blade shape from a known airfoil type for an optimum rotor means determining the blade shape parameters; chord length distribution and twist distribution along the blade length for a certain tip-speed ratio at which the power coefficient of the rotor is maximum. Therefore first of all the change of the power coefficient of the rotor with respect to tip-speed ratio should be figured out in order to determine the design tip-speed ratio, corresponding to which the rotor has a maximum power coefficient

Aerodynamic Behavior of Aerofoil

Airfoils for horizontal axis wind turbines (HAWT) are designed to be used at low angle of attack, where the lift coefficient is high and drag coefficient are fairly low.

Aerodynamic Performance

The primary aerodynamic factors affecting blade design are:

- design rated power and rated wind speed;
- design tip speed ratio;
- solidity;
- airfoil;
- number of blades;
- rotor power control (stall or variable pitch);
- Rotor orientation (upwind or downwind of the tower).

The overall size of the rotor swept area, and hence the Length of the blades, is directly related to design rated power and rated wind speed. Other things being equal, it is usually advantageous to have a high design tip speed ratio. A high tip speed ratio results in a low solidity, which in turn results in less total blade area. This, in turn, should result in lighter, less expensive blades. The accompanying higher rotational speed is also of benefit to the rest of the drive train. On the other hand, high tip speed ratios result in more aerodynamic noise from the turbine. Because the blades are thinner, the flap wise stresses tend to be higher. Thinner blades are also more flexible.

Structural Strength

The exterior shape of wind turbine blades is based on aerodynamics, but the interior architecture is determined primarily by considerations of strength.

The blade structure must be sufficiently strong both to withstand extreme loads and to survive many fatigue cycles.

The blade must also not deflect more than a specified amount when under load.

Key structural design requirements

- The blades must be strong to resist the extreme (ultimate) loads;
- The blades must resist the time-varying (fatigue) loads through the entire life of the blade;
- The blades must be stiff to prevent collision with the tower under extreme loads. Local stiffness must be also sufficient to prevent instability of components under compression (to avoid local or global buckling)
- The blade construction needs to be as light as possible to minimize the cost of generated power
- The blades should be stiff and light to avoid resonance

The structural design requirements translate to the following materials requirements in terms of material properties:

- ✓ **High material strength** is needed to withstand the extreme loads
- ✓ **High fatigue strength** is needed to resist varying loads and reduce material degradation during service
- ✓ **High material stiffness** is needed to maintain aerodynamic shape of the blade, to prevent collision with the tower, and to prevent local instability (buckling) under compressive loads
- ✓ **Low density** is needed to reduce gravity forces and to minimize the cost of power

Materials requirements

Many types of materials are used in wind turbines, as summarized in figure below. Two of the most important of these are steel and composites.

The composites typically comprise fiberglass, carbon fibers, or wood together with a matrix of polyester or epoxy. Other common materials include copper and concrete.

Table 1: materials used in wind turbines

Subsystems or components	Material category	Material subcategory
Blades	Composites	Glass fibers, carbon-fibers, wood laminates, polyesters risen epoxy
Hub	Steel	
Gearbox	Steel	Various alloys, lubricants
Generator	Steel, copper	Rare earth based permanent magnets
Mechanical equipment	steel	
Nacelle cover	composites	Fiber glass
Tower	steel	
Foundation	Steel, concrete	
Electrical and control system	Copper silicon	

Based on this modeling is done by taking a standard wind blade data from AID (airfoil investigation database). And from the data AH 79-100 C and GOE 239 (MVA H.31) AIRFOIL are taken and by comparing their parameter airfoil can develop the model by tracing or taking DAT file to x y z coordinate to

SOLIDWORKS 2019 and develop the model by tracing

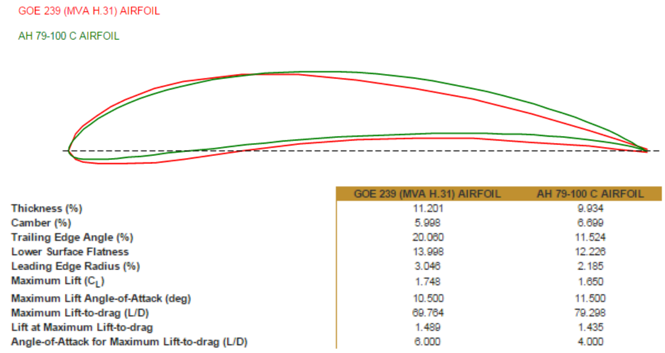

	GOE 239 (MVA H.31) AIRFOIL	AH 79-100 C AIRFOIL
Thickness (%)	11.201	9.934
Camber (%)	5.998	6.699
Trailing Edge Angle (%)	20.060	11.524
Lower Surface Flatness	13.998	12.226
Leading Edge Radius (%)	3.046	2.185
Maximum Lift (C_L)	1.748	1.650
Maximum Lift Angle-of-Attack (deg)	10.500	11.500
Maximum Lift-to-drag (L/D)	69.764	79.298
Lift at Maximum Lift-to-drag	1.489	1.435
Angle-of-Attack for Maximum Lift-to-drag (L/D)	6.000	4.000

Figure 10: comparing of the two airfoils

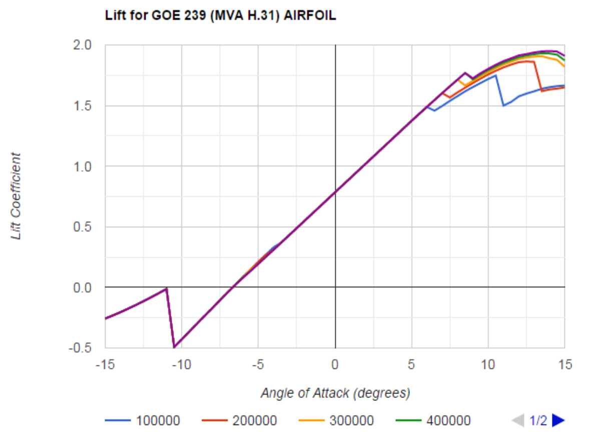

Figure 11 GOE 239 (MVA H.31 lift coefficient Vs angle of attack

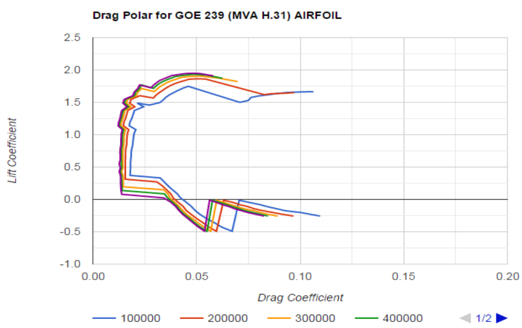

Figure 12 Lift VS Drag coefficient

Based on efficiency characteristics GOE 239 (MVA H.31) has maximum 52.2 > 43.8 and also comparing other parameters the selection airfoil is GOE 239 (MVA H.31)

Figure 13: 3D model of the blade by SOLIDWORKS 2019

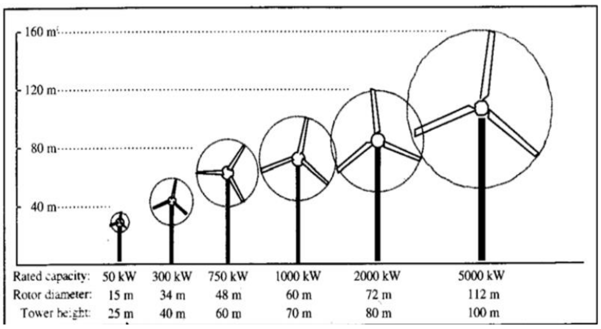

Figure 14 rated capacity, rotor diameter, and tower height for turbines

Table 2: typical wind turbine sizes as design data

Tower height (m)	Rotor diameter (m)	Rated power (kw)
22	21	55
31	30	225
35	35	450
35-40	41-44	500
44	43	600
50	48	750
50	54	1000
60	58	1500
64-80	72-76	2000
85	115	5000

Analytical Solution

Generalized Rotor Design Procedure

Determine Basic Rotor Parameters

1. Begin by deciding what power, P, is needed at a particular wind velocity, U. Include the effect of a probable CP and radius, R of various other components (e.g. gearbox, generator, pump, etc.). efficiencies, η of the, of the rotor may be estimated from

$P = C_p\eta(\frac{1}{2})\rho\pi R^2 U^3$ *Equation 8*

Consider that the net power to be 2MW

$\eta = \eta_m * \eta_e$ *Equation 9*

Annual mean wind velocity

This value is mainly consider the Ethiopian maximum mean wind velocity for turbine IEC class II

$$vmean = 8.5\frac{m}{s}$$

$vdesign = 1.4vmean\ldots\ldots\ldots\ldots\ldots\ldots$ *Equation 10*

$$vdesign = 11.9 \approx 12m/s$$

$$2e^6 = 47\% * \eta * 0.5 * 1.225 * \pi * 36^2 * 12^3$$

$$\eta = 0.98$$

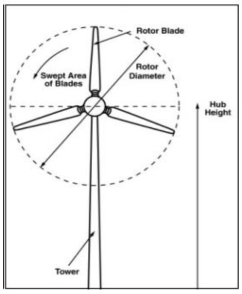

Figure 15: swept area and hub height

The swept area

$$A = \pi \frac{D^2}{4} = \pi R^2 \ldots\ldots\ldots\ldots\ldots\ldots\ldots\ldots\ldots .Equation\ 11$$

$$A = 4071.5\ m^2$$

Power in the air

$$p_w = 0.5 \rho A v^3 \ldots\ldots\ldots\ldots\ldots\ldots\ldots\ldots .Equation\ 12$$

$$p_w = 430275.6\ watts$$
$$= 4.3MW$$
$$but\ \ at\ H$$

$$\rho = \rho_0 - 1.994 * 10^{-4} * H \ldots\ldots\ldots\ldots\ldots .Equation\ 13$$

$$1.225 - 1.994 * 10^{-4} * 80$$

$= 1.210672$ kg/m^3

$$p_w = 4258872.905\ watts$$
$$= 4.25MW$$

Power of blade

By taking the theoretical efficiency range of wind power from range and taking 0.47

$$p_{blade} = c_p * p_w \eta\ \ldots\ldots\ldots\ldots\ldots .Equation\ 14$$

$$p_{blade} = 2.0825MW$$

The efficiency of energy transformation in turbine

$$\eta = \frac{p_{blade}}{p_w} \ldots\ldots\ldots\ldots .Equation\ 15$$

$$\eta = 0.4755 \approx 0.48$$

2. According to the type of application, choose a tip speed ratio, λ. For a water-pumping windmill, for which greater torque is needed, use 1 < λ < 3. For electrical power generation, use 4 < λ < 10. The higher speed machines use less material in the blades and have smaller gearboxes, but require more sophisticated airfoils

Table 3 suggested blade number, B for different tip speed ratio

B	λ
8-24	1
6-12	2
3-6	3
3-4	4
1-3	>4

3. Choose the number of blades, B, from Table 1. Note: if fewer than three blades are selected, there are a number of structural dynamic problems that must be considered in the hub design
4. Select an airfoil. If λ < 3, curved plates can be used. If λ > 3, use a more aerodynamic shape. This implies that for B= 1-3 tip speed ratio λ is greator than 4 this implies the design is more aerodynamic

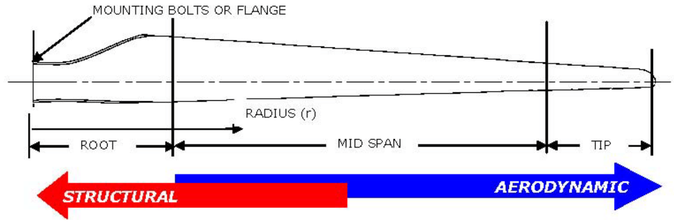

Figure 16 structural and aerodynamic parts of a rotor blade

Define the Blade Shape

5. Obtain and examine the empirical curves for the aerodynamic properties of the airfoil at each section (the airfoil may vary from the root to the tip)

6. Divide the blade into N elements (usually 10–20). Use the optimum rotor theory to estimate the shape of the ith blade with a midpoint radius

A high tip speed ratio results low solidity which in turn results in less total blade area this in turn should result in lighter less expensive blade.

In accompanying higher rotational speed is also of benefit in the rest of the drive train

High tip speed ration result in more aerodynamic noise from the turbine because blades are thinner this implies the flap wise stresses tend to higher at design tip speed ratios increases selection of proper. Wind turbines are rotating machines, and a very important dimensionless number is the tip speed ratio (TSR) defined as

$$\lambda = \frac{v_{TIP}}{v_{WIND}} = \frac{\omega.R}{v} \ldots\ldots .Equation\ 16$$

take λ as 7 from table

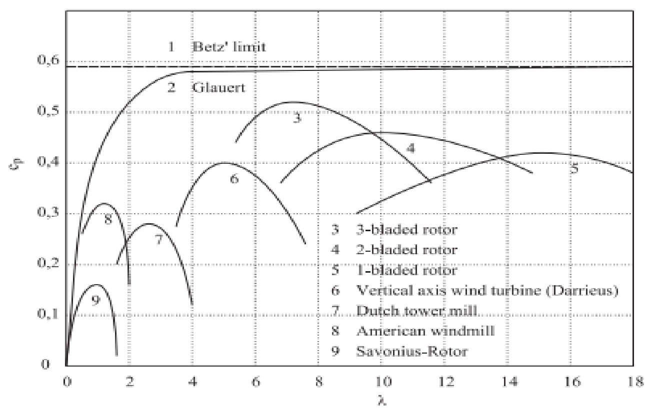

Figure 17 C_P as function of TSR, various types of wind turbines

$$\omega = \frac{\lambda v}{R} = 7 * \frac{12}{36}$$

$$= 2.33\ \frac{rad}{s}$$

$$\omega = \frac{2\pi N}{60} \ldots\ldots\ldots\ldots\ldots .Equation\ 17$$

$$N = \omega * \frac{60}{2\pi} = 22.28 \approx 22\ rpm$$

$$Rotor\ torque = \frac{p_{blade}}{\omega} \ldots\ldots\ldots Equation\ 18$$

$$Rotor\ torque = \frac{2.0825MW}{2.5}$$

$$= 833 \left(\frac{KN}{m}\right)$$

$$total\ thrust = \frac{1}{2}\rho A v^2 \ldots\ldots\ldots\ldots Equation\ 19$$

$$= 0.5 * 1.210672 * 4071.5 * 12^2$$

$$= 354.9\ KN$$

$$thurst = C_T * total\ thrust$$

$$= \frac{C_p}{\lambda} * total\ thrust$$

$$= 0.063 * 354.9KN$$

$$= 22359.08N$$

$$\varphi = tan^{-1}\left(\frac{2}{3\lambda_r}\right) \ldots\ldots\ldots\ldots Equation\ 20$$

$$\lambda_r = \lambda\left(\frac{r}{R}\right) \ldots\ldots\ldots\ldots Equation\ 21$$

Where λ is tip speed ratio and $\frac{r}{R}$ is elemental section radius R Rotor radius

By taking $\frac{r}{R} = 0.5$

$$= 7 * 0.5 = 3.5$$

$$\varphi = \tan^{-1}\left(\frac{2}{3 * 3.5}\right)$$

$$= 10.78 \approx 10.8\ degree\quad but$$

$$\varphi = \theta_p + \alpha \ldots\ldots\ldots\ldots Equation\ 22$$

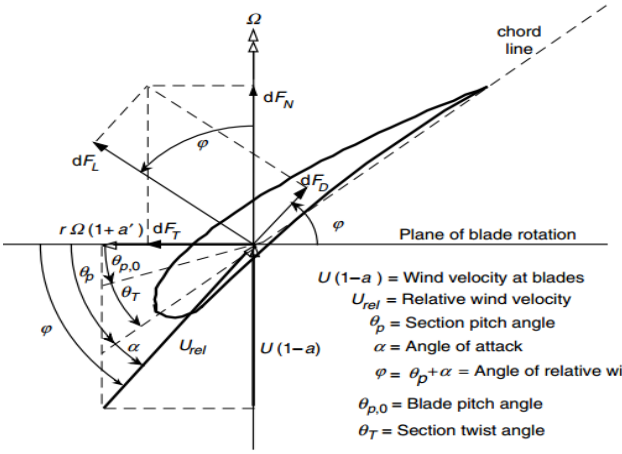

Figure 18: blade aerofoil resolving relations

Table 4 19 twist and chord distribution for the example Betz optimum blade r/R, fraction of rotor radius; C/R, non- dimensionalized chord

r/R	c/R	Twist angle (deg)	Angle of rel. wind (deg)	Section pitch (deg)
0.1	0.275	38.2	43.6	36.6
0.2	0.172	20.0	25.5	18.5
0.3	0.121	12.2	17.6	10.6
0.4	0.092	8.0	13.4	6.4
0.5	0.075	5.3	10.8	3.8
0.6	0.063	3.6	9.0	2.0
0.7	0.054	2.3	7.7	0.7
0.8	0.047	1.3	6.8	−0.2
0.9	0.042	0.6	6.0	−1.0
1	0.039	0	5.4	−1.6

$$\frac{r}{R} = 0.5, \frac{C}{R} = 0.075$$

$$twist\ angle = 5.3$$

$$angle\ of\ relative\ wind = 10.8$$

$$section\ pitch\ angle = 3.8$$

$$c_{p=}4a(1-a)^2 \ \ldots\ldots\ldots Equation\ 23$$

From this equation by using MATLAB software and $c_{p=}0.47$ the square roots are

$$a = 0.1175$$

The chord distribution of aerofoil

$$C = \frac{8\pi r sin\varphi}{3Bc_l\lambda_r} \ldots\ldots\ldots\ldots Equation\ 24$$

$$= \frac{8 * \pi * 36 * sin10.8}{3 * 3 * 1 * 3.5}$$

$$= 5.38$$

$$tan\,\varphi = \frac{1-a}{(1+a')\lambda_r} \ \ldots\ldots\ldots\ldots Equation\ 25$$

$$from\ above\ \ equation\ a' = 0.321$$

$$solidity$$

A disadvantage of such a high-solidity rotor is the excessive forces that it will attract during extreme wind speeds such as in hurricanes.

$$\sigma = \frac{Bc}{2\pi r} \ldots\ldots\ldots\ldots Equation\ 26$$

$$\sigma = \frac{3 * 5.382}{2 * \pi * 36} = 0.07138$$

Tip Loss: Effect on Power Coefficient of Number of Blades

A number of methods have been suggested for including the effect of the tip loss. The most straightforward approach to use is one developed by Prandtl (see de Vries, 1979). This correction factor is a function of the number of blades, the angle of relative wind, and the position on the blade. Based on Prandtl's method:

$$\boldsymbol{F_i = (2/\pi)\cos^{-1}[\exp[\frac{-(B/2)[1-(r_i/R)]}{(r_i/R)\sin\varphi_{opt,i}}]]} \ldots$$

$$F = 0.998064834$$

Where the angle resulting from the inverse cosine function is assumed to be in radians. If the inverse cosine function is in degrees, then the initial factor,$2/\pi$ is replaced by$1/90$. Note, also, that F is always between 0 and 1. This tip loss correction factor characterizes the reduction in the forces at a radius r along the blade that is due to the tip loss at the end of the blade.

$there\ fore\ 0 < F < 1$

$0 < 0.998064834 < 1$

$C_L = \frac{4\sin\varphi}{\sigma}\ (\frac{\cos\varphi - \lambda_r\sin\varphi}{\sin\varphi + \lambda_r\cos\varphi})$ ……*Equation 27*

Inserting calculated values

$$C_L = 0.9426 \approx 1$$

$$C = \frac{8\pi r}{3Bc_l}(1 - \cos\varphi)$$

$the\ same\ value\ \ C = 5.38\ calculated\ above$

From Rotor power which defined as product of the torque due to the drag force and rotational speed of rotor surface

$P = C_D[\frac{1}{2}\rho A(U - \Omega r)^2]\Omega r$.....*Equation 28*

$= (\rho AU^3[\frac{1}{2}C_D\lambda(1-\lambda)^2]$……*Equation 29*

From above equation we solve the drag coefficient

$$C_D = 2.96 * 10^{-3}$$

The drag force, FD, is a function of the relative wind velocity at the rotor surface (the difference between the wind speed, U, and the speed of the surface,Ωr)

$F_D = C_D[\frac{1}{2}\rho(U - \Omega r)^2 A]$………*Equation 30*

Where A is the drag surface area and where the three-dimensional drag coefficient, C_D

Therefore drag force

$$F_D = 44481.56N\ \mathrm{N}$$

The forces in lift machines are also a function of the relative wind velocity and of the lift coefficient

$F_L = C_L(\frac{1}{2}\rho AU_{rel}^2)$……………*Equation 31*

Table 5the IEC turbine classes

Classes	I	II	III	IV
U_{ref}	50	42.5	37.5	30
U_{av}	10	8.5	7.5	6

Relative velocity

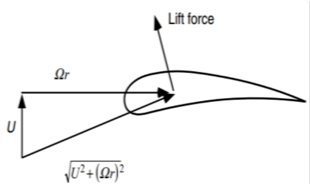

Figure 20: velocity resolving

$U_{rel} = \sqrt{U^2 + (\Omega r)^2} = U\sqrt{1+\lambda^2}$………*Equation 32*

$$U_{rel} = 12\sqrt{1+7^2}$$
$$= 12\sqrt{50}$$
$$= 84.85\ m/s$$

or

$$\mathrm{U_{rel}} = \sqrt{12^2 + (2.33 * 36)^2}$$
$$\mathrm{U_{rel}} = \sqrt{144 + (83.88)^2}$$
$$\mathrm{U_{rel}} = \sqrt{7179.8544}$$
$$=84.73m/s$$

Inserting from above equation

$$F_L = 20319950N$$

Structural load on wind turbine

$$A = F_L\cos\varphi + F_D\sin\varphi$$

$$= 19968363N$$

Driving force

$$R = F_L\sin\varphi - F_D\cos\varphi$$

$$= 3763885N$$

Wind power density

The wind power per unit area, P/A or wind power density is:

$$\frac{P}{A} = \frac{1}{2}\rho U^3$$

$$= 0.5 * 1.225 * 12^3$$

$$= 1046\ \mathrm{W}/m^2$$

One should note that:

- The wind power density is proportional to the density of the air. For standard conditions (sea-level, 15degree Centigrade) the density of air is 1.225 kg/m^3.

- Power from the wind is proportional to the area swept by the rotor (or the rotor diameter squared for a conventional horizontal axis wind machine).
- The wind power density is proportional to the cube of the wind velocity.
- The actual power production potential of a wind turbine must take into account the fluid mechanics of the flow passing through a power-producing rotor, and the aerodynamics and efficiency of the rotor/generator combination.
- In practice, a maximum of about 45% of the available wind power is harvested by the best modern horizontal axis wind turbines

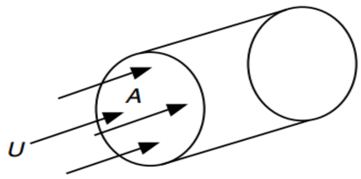

Figure 21 flow of air through a rotor disc A, area,U wind velocity

Table 6power per unit area available from steady wind (density=1.225 kg/m^3)

Wind speed (m/s)	Power/Area(W/m^2)
0	0
5	80
10	610
15	2070
20	4900
25	9560
30	16550

Some sample qualitative magnitude evaluations of the wind resource are

Table 7 wind power density prediction

Wind power density	Value	Prediction
P/A	$< 100\ \mathrm{W}/m^2$	Low
P/A	$\approx 400\ \mathrm{W}/m^2$	Good
P/A	$> 700\,\mathrm{W}/m^2$	Great

From table we can deduce that the design is great.

$$1046\,\mathrm{W}/m^2 > 700\,\mathrm{W}/m^2$$

Rotor blade as beam element

Beam theory applies when one of the dimensions of the structure is much larger than the others Using asymptotic analysis, it is possible to eliminate the dependence on the two shortest dimensions by appropriate averaging of the distributed elastic Beam theory considers combined bending, tension and torsion. There are several beam models of varying complexity. The simplest is the first order or Euler Bernoulli model in which the elastic axis is considered rectilinear while cross sections originally normal to it remain so in the deformed state. As a consequence shear is eliminated.

There are three steps to take:

- Define the deformation kinematics,
- Introduce the stress–strain relations,
- Apply dynamic equilibrium to a differential volume of the structure

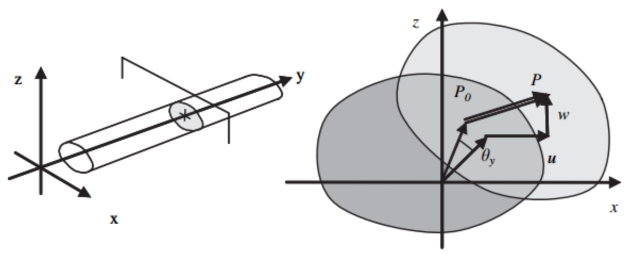

Figure 22 deformation of a beam cross section

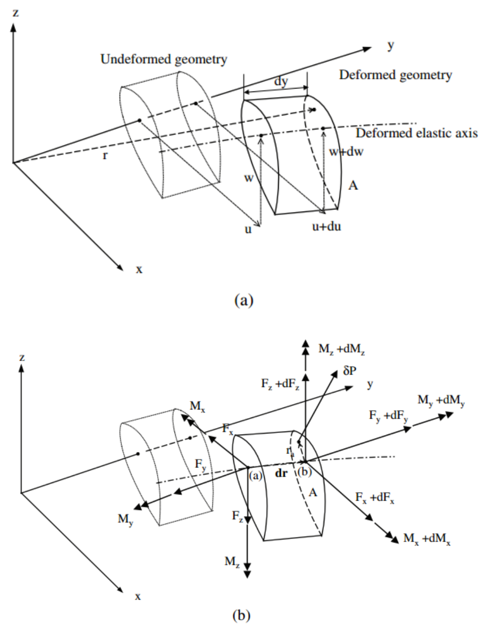

Figure 23: loads and displacements of a beam element

The beam element is a two-dimensional finite element where the local and global coordinates coincide. It is characterized by linear shape functions. The beam element has modulus of elasticity *E*, moment of inertia *I*, and length *L*. Each beam element has two nodes and is assumed to be horizontal as shown in Fig. In this case the element stiffness matrix is given by the following matrix, assuming axial deformation is neglected

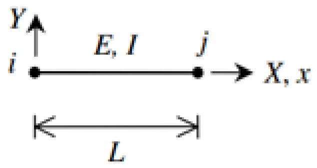

Figure 24 the beam element

$$K = \frac{EI}{L^3}\begin{bmatrix} 12 & 6L & -12 & 6L \\ 6L & 4L^2 & -6L & 2L^2 \\ -12 & -6L & -12 & -6L \\ 6L & 2L^2 & -6L & 4L^2 \end{bmatrix} \ldots\ldots \textit{Equation 33}$$

It is clear that the beam element has four degrees of freedom two at each node (a transverse displacement and a rotation).

The sign convention used is that the displacement is positive if it points upwards and the rotation is positive if it is counterclockwise. Consequently for a structure with n nodes, the global stiffness matrix K will be of size 2 n × 2 n (since we have two degrees of freedom at each node). The global stiffness matrix K is assembled by making calls to the MATLAB function BeamAssemble which is written specifically for this purpose Once the global stiffness matrix K is obtained we have the following structure equation:

$$[K]\{U\} = \{F\} \ldots \textit{Equation 34}$$

Where U is the global nodal displacement vector and F is the global nodal force vector. At this step the boundary conditions are applied manually to the vectors U and F. Then the matrix is solved by partitioning and Gaussian elimination. Finally once the unknown displacements and reactions are found, the nodal force vector is obtained for each element as follows:

$$\{f\} = [K]\{u\} \ldots. \textit{Equation 35}$$

Where *{f}* is the 4 × 1 nodal force vector in the element and *u* is the 4 × 1 element displacement vector. The first and second elements in each vector $\{u\}$ are the transverse displacement and rotation, respectively, at the first node, while the third and fourth elements in each vector $\{u\}$ are the transverse displacement and rotation, respectively, at the second node.

Blade bending moment

It can be seen that the upper longitudinal fibres of the beam are compressed while the lower fibres are stretched. It follows that between these two extremes there is a fibre that remains unchanged in length. Thus the direct stress varies through the depth of the beam from compression in the upper fibres to tension in the lower. Clearly the direct stress is zero for the fibre that does not change in length. The surface that contains this fibre and runs through the length of the beam is known as the neutral surface or neutral plane; the line of intersection of the neutral surface and any cross-section of the beam is termed the neutral axis.

The problem, therefore, is to determine the variation of direct stress through the depth of the beam, the values of the stresses and subsequently to find the corresponding beam deflection.

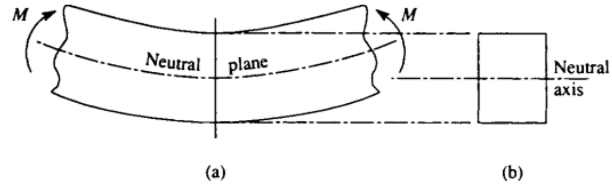

Figure 25: beam deflection at neutral axes

Assumptions

the primary assumption made in determining the direct stress distribution produced by pure bending is that plane cross-sections of the beam remain plane and normal to the longitudinal fibres of the beam after bending. We shall also assume that the material of the beam is linearly elastic, i.e. it obeys Hooke’s law, and that the material of the beam is homogeneous.

Considering as a simple cantilever

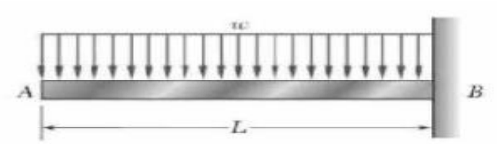

Figure 26: a simple cantilever beam with distributed load

We can calculate the reaction and moment forces at any point by

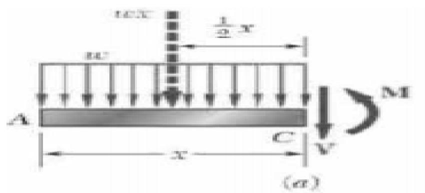

Figure 27: reaction, bending and shear forces

$$\uparrow \sum F_y = 0\!:\; -wx - V = 0 \; V = -wx .. \textit{Equation 36}$$

$$\uparrow \sum M_y - 0 : \; wx\left(\frac{x}{2}\right) + M - 0 \quad M = \frac{1}{2}wx^2 \ldots \textit{Equation 37}$$

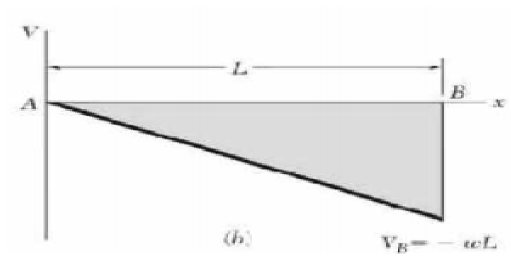

Figure 28: maximum shear force diagram

$$V_B = -wL, M_B = -\frac{1}{2}wL^2 \ldots\ldots \textit{Equation 38}$$

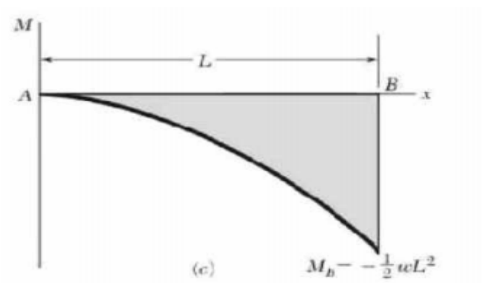

Figure 29: maximum bending moment diagram

IJISET - International Journal of Innovative Science, Engineering & Technology, Vol. 6 Issue 5, May 2019
ISSN (Online) 2348 – 7968
www.ijiset.com

For this the studied value is based on blade own weight and atmospheric pressure load

Bending by its own load

For 2MW wind turbine each blade weighs about 6.2 ton this implies that 608220 N is its own load the matlab program gives the following value

Table 8: MATLAB 2018b output value

Length of beam in meter	36
Type 1 for point load, Type 2 for udl Load case	2
Uniformly distributed load in (kN/m)	60.8
Length of udl in meter	36
C.G of udl from left end of the beam in meter	10
Left support Reaction (KN)	1580.8
Right support Reaction (kN)	608
Maximum bending moment (kNm)	7904

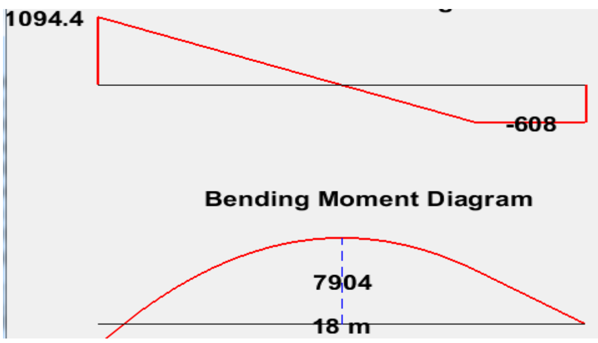

Figure 30: Shear Force Diagram and bending moment diagram MATLAB 2018b output

Bending moment due to atmospheric pressure

Table 9 MATLAB 2018b output value

Length of beam in meter	36
Type 1 for point load, Type 2 for udl Load case	2
Uniformly distributed load in (kN/m)	101.3
Length of udl in meter	36
C.G of udl from left end of the beam in meter	10
Left support Reaction (KN)	2633.8
Right support Reaction (KN)	1013
Maximum bending moment (kNm)	13169

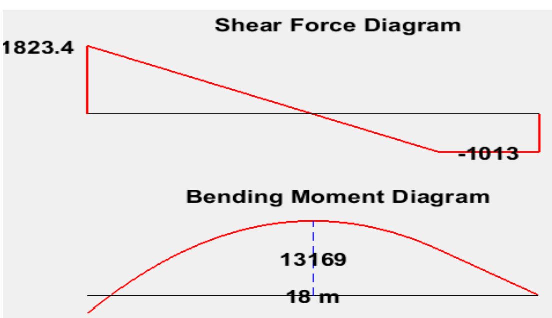

Figure 31: Shear Force Diagram and bending moment diagram MATLAB 2018b output

Maximum stress due to gravity

$$\sigma_g = \frac{W r_{cg}\left(\frac{c}{2}\right)}{I} = \frac{\frac{W r_{cg}}{tc^2}}{6}$$

Where W= weight of blade

r_{cg} =center of gravity

c= camber

t = thickness

Assume that t=c I= 12.9767

$$\sigma_g = 8600$$

Stress due to centrifugal force

$$\sigma_g = {}^{F_c}/_{A_c}$$

$$F_c = \frac{W r_{cg} * \Omega^2}{g}$$

$$F_c = 5479N$$

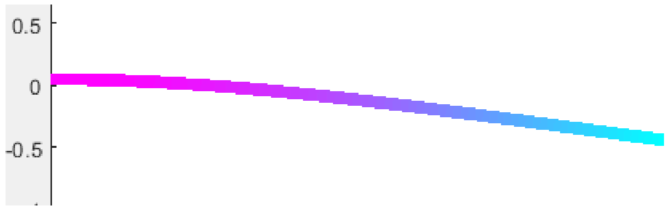

Figure 32: blade deflection considering as simple cantilever beam

$MATLAB\ 2018b^R$ and $SOLIDWORK\ 2019\ ^R$ simulations

Having the above calculated values we come up to $MATLAB\ 2018b^R$ and $SOLIDWORK\ 2019\ ^R$ as follows

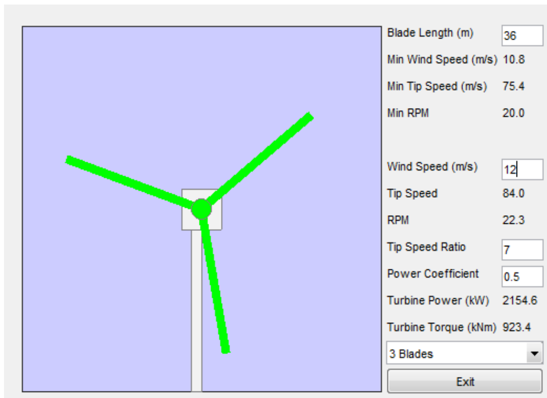

Figure 33 $MATLAB\ 2018b^R$ tip speed, turbine power and torque output

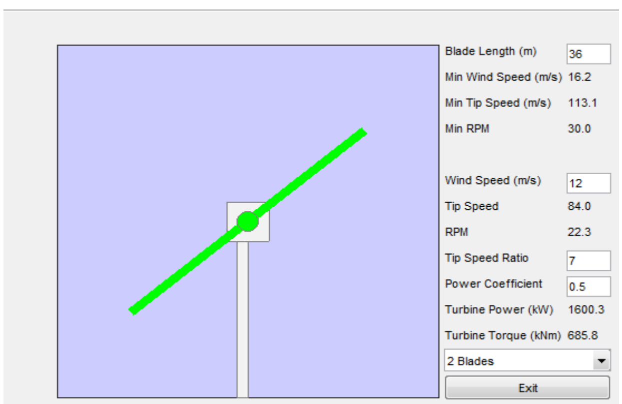

IJISET - International Journal of Innovative Science, Engineering & Technology, Vol. 6 Issue 5, May 2019
ISSN (Online) 2348 – 7968
www.ijiset.com

Figure 34 comparisons between power and torque @ B=2, 3, 4, 5

Comparison of each value in the above different situation based on blade numbers except blade number two others give the same value but from design point of view the increase of blade number we can see the following consequence's

Table 10 turbine torque and turbine power comparisons

Blade number	Turbine power(KW)	Turbine torque(KNm)
2	1600.3	685.8
3	2154.6	923.4
4	2154.6	923.4
5	2154.6	923.4

Table 11: comparison based on design view

Blade number	2	3	Multiple
Torque	Low	High	High torque
RPM	High	Lower	Low
Power	Same	Same	Same
Noise	More	Less	No
View	Less esthetic	Esthetic	Esthetic
cost	Cheap		Expensive
Application	Offshore	onshore	Wind pumps

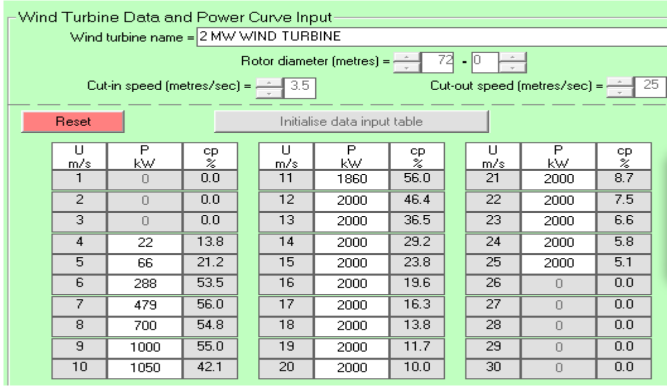

U m/s	P kW	cp %	U m/s	P kW	cp %	U m/s	P kW	cp %
1	0	0.0	11	1860	56.0	21	2000	8.7
2	0	0.0	12	2000	46.4	22	2000	7.5
3	0	0.0	13	2000	36.5	23	2000	6.6
4	22	13.8	14	2000	29.2	24	2000	5.8
5	66	21.2	15	2000	23.8	25	2000	5.1
6	288	53.5	16	2000	19.6	26	0	0.0
7	479	56.0	17	2000	16.3	27	0	0.0
8	700	54.8	18	2000	13.8	28	0	0.0
9	1000	55.0	19	2000	11.7	29	0	0.0
10	1050	42.1	20	2000	10.0	30	0	0.0

Figure 35 wind turbine power and curve input

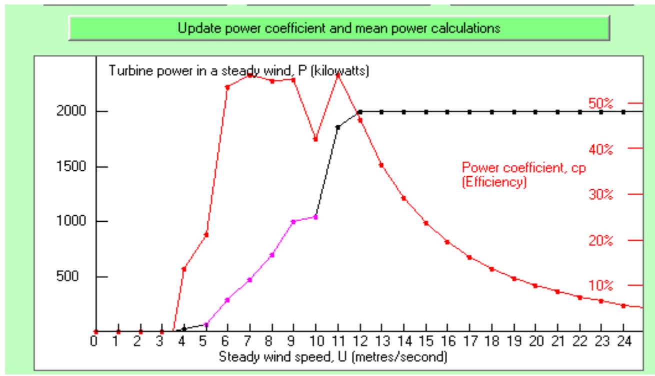

Figure 36 power coefficient and mean power calculation

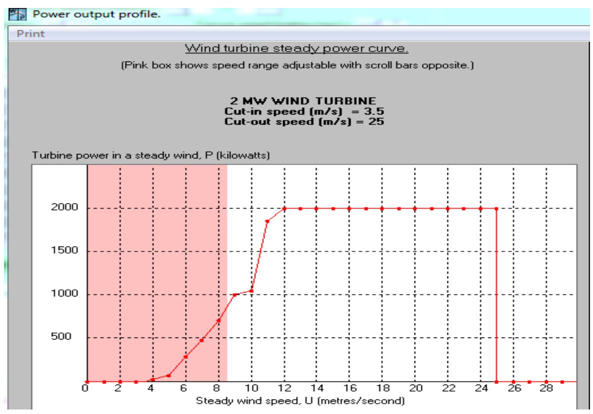

Figure 37: designed turbine power curve

Solidwork blade static simulation

The software uses the Finite Element Method (FEM). FEM is a numerical technique for analyzing engineering designs. FEM is accepted as the standard analysis method due to its generality and suitability for computer implementation. FEM divides the model into many small pieces of simple shapes called elements effectively replacing a complex problem by many simple problems that need to be solved simultaneously.

Elements share common points called nodes. The process of dividing the model into small pieces is called meshing.
The behavior of each element is well-known under all possible support and load scenarios. The finite element method uses elements with different shapes.

The response at any point in an element is interpolated from the response at the element nodes. Each node is fully described by a number of parameters depending on the analysis type and the element used. For example, the temperature of a node fully describes its response in thermal analysis. For structural analyses, the response of a node is described, in general, by three translations and three rotations. These are called degrees of freedom (DOFs). Analysis using FEM is called Finite Element Analysis (FEA).

Mesh property

Figure 38: blade meshing

Reaction forces

Selection set	**Units**	**Sum X**	**Sum Y**	**Sum Z**	**Resultant**
Entire Model	N	-776.688	-62.3438	876.893	1,173.06

Results

Name	Type	Min	Max
Stress1	VON: von Mises Stress	2.480e-02 N/mm^2 (MPa) Node: 2822	7.815e+03 N/mm^2 (MPa) Node: 173

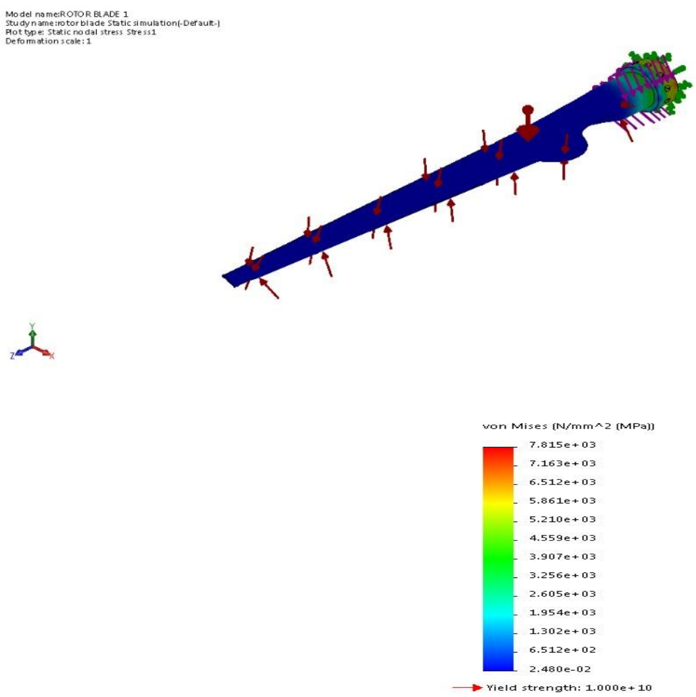

Figure 39: static stress analysis

Name	Type	Min	Max
Displacement1	Resultant Displacement	0.000e+00 mm Node: 384	1.861e-05 mm Node: 1385

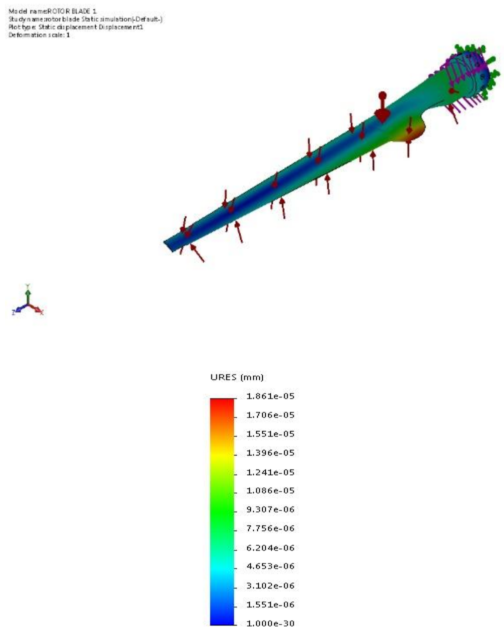

Figure 40: static displacement analysis

Name	Type	Min	Max
Strain1	ESTRN: Equivalent Strain	1.806e-13 Element: 37551	7.623e-08 Element: 14922

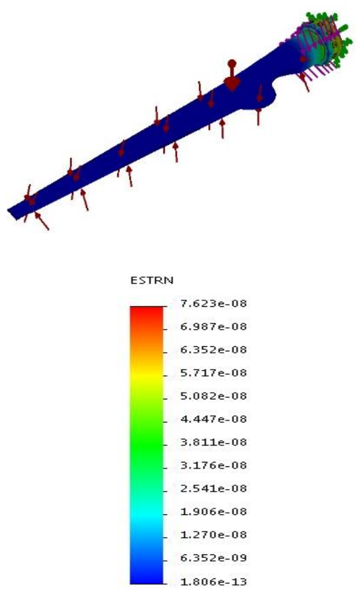

Figure 41: static strain analysis

Creep study

When loads are applied to a body, the body deforms and the effect of loads is transmitted throughout the body. The external loads induce internal forces and reactions to render the body into a state of equilibrium.

Linear Static analysis calculates displacements, strains, stresses, and reaction forces under the effect of applied loads.

Selection set	*units*	*Sum X*	*Sum Y*	*Sum Z*	*resultant*
Entire node	*N*	*-0.490416*	*0.00208795*	*11.1378*	*11.178*

Name	Type	Min	Max
Stress1	VON: von Mises Stress at Step No: 1(3.7626e-315 Seconds)	0.000e+00 N/m^2 Node: 15	1.429e+04 N/m^2 Node: 3363

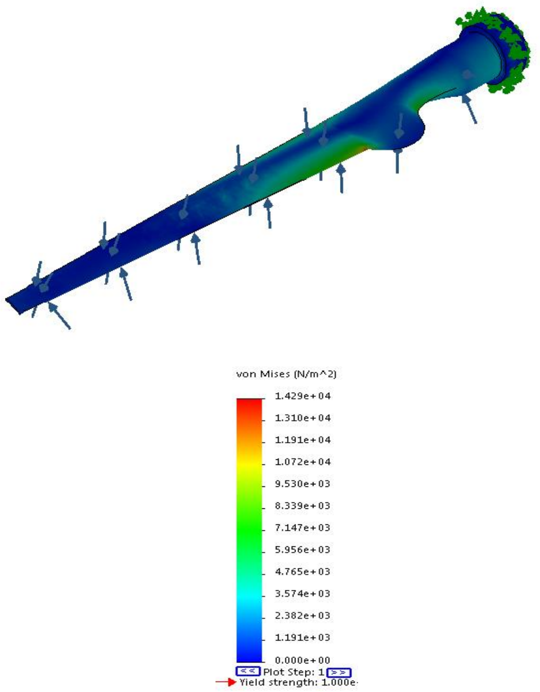

Figure 42: stress analysis

Name	Type	Min	Max
Displacement1	URES: Resultant Displacement at Step No: 1(3.7626e-315 Seconds)	0.000e+00 mm Node: 1	9.619e-10 mm Node: 4838

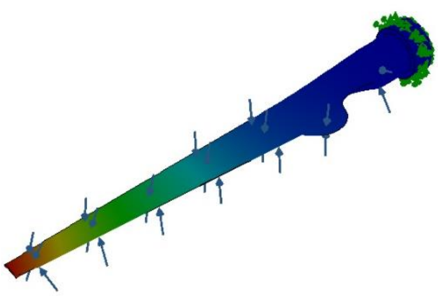

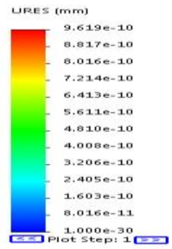

Figure 43: displacement analysis

Name	Type	Min	Max
Strain1	ESTRN:Equivalent Strain at Step No:100(3.7626e-315 Seconds)	0.000e+00 Element: 8062	1.621e-11 Element: 13074

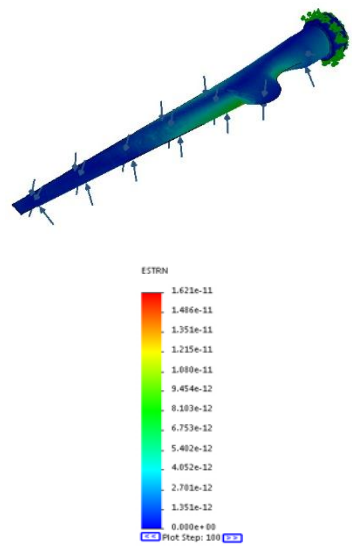

Figure 44: strain analysis

Fatigue analysis

Wind turbines, by their very nature, are subject to a great number of cyclic loads. The lower bound on the number of many of the fatigue-producing stress cycles in turbine components is proportional to the number of blade revolutions over the turbine's lifetime. The total cycles, nL, over a turbine's lifetime would be

$$n_L = 60\ kn_{rotor}H_{op}Y$$

Where

k is the number of cyclic events per revolution. n_{rotor}, is the rotational speed of rotor (rpm).

H_{op}, is the operating hours per year and.

Y is the years of operation.

For blade root stress cycles, k would be at least equal to 1 while, for the drive train or tower, k would be at least equal to the number of blades. A turbine with an rpm of approximately 30 operating 4000 hours per year would experience more than 108 cycles over a 20-year lifetime. This may be compared to many other manufactured items, which would be unlikely to experience more than 106 cycles over their lifetime. In fact, the number of cyclic events on a blade can be much more than once per revolution of the rotor. It is observed that repeated loading and unloading weakens objects over time even when the induced stresses are considerably less than the allowable stress limits. This phenomenon is known as fatigue. Each cycle of stress fluctuation weakens the object to some extent. After a number of cycles, the object becomes so weak that it fails. Fatigue is the prime cause of the failure of many objects, especially those made of metals. Examples of failure due to fatigue include, rotating machinery, bolts, airplane wings, consumer products, offshore platforms, ships, vehicle axles, bridges, and bones.

Linear and nonlinear structural studies do not predict failure due to fatigue. They calculate the response of a design subjected to a specified environment of restraints and loads. If the analysis assumptions are observed and the calculated stresses are within the allowable limits, they conclude that the design is safe in this environment regardless of how many times the load is applied.

Results of static, nonlinear, or time history linear dynamic studies can be used as the basis for defining a fatigue study. The number of cycles required for fatigue failure to occur at a location depends on the material and the stress fluctuations. This information, for a certain material, is provided by a curve called the SN curve.

Stages of Failure Due to Fatigue

Failure due to fatigue occurs in three stages:

1. One or more cracks develop in the material. Cracks can develop anywhere in the material but usually occur on the boundary faces due to higher stress fluctuations. Cracks can occur due to many reasons. Imperfections in the microscopic structure of the materials and surface scratches caused by tooling or handling are some of them.
2. Some or all the cracks grow as a result of continued loading.
3. The ability of the design to withstand the applied loads continue to deteriorate until failure occurs

Fatigue cracks start on the surface of a material. Strengthening the surfaces of the model increases the life of the model under fatigue events.

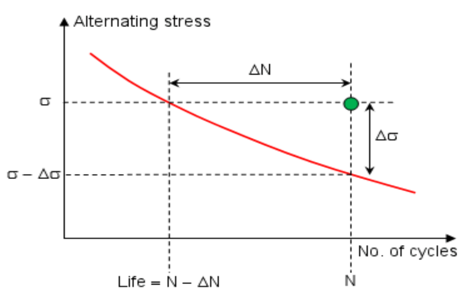

Figure 45: alternating stress Vs No of cycle

Name	Type	Min	Max
Results1	Damage plot	1.000e-01 Node: 1	1.000e-01 Node: 1

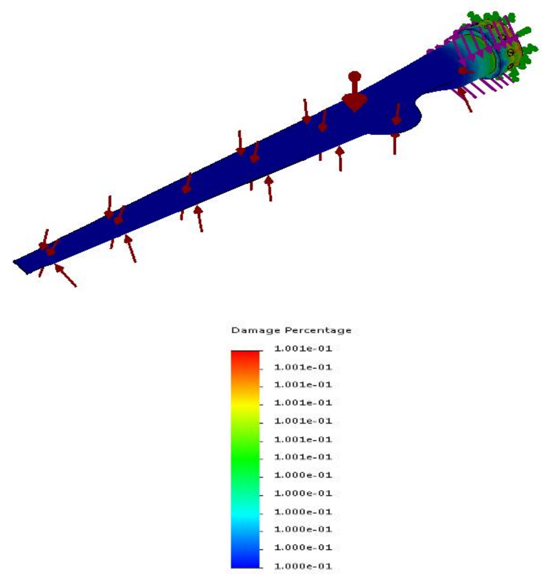

Figure 46: damage percentage

Name	Type	Min	Max
Results2	life plot	1.000e+06 cycle Node: 1	1.000e+06 cycle Node: 1

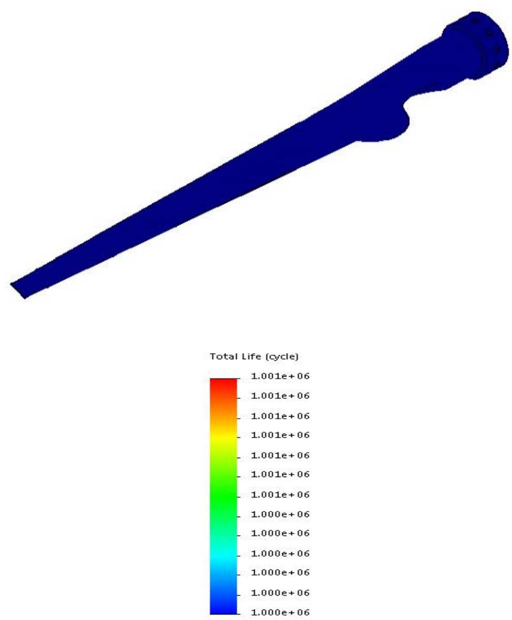

Figure 47: total life (cycle)

Name	Type	Min	Max
Results3	Load factor	2.201e+07 Node: 173	1.909e+11 Node: 2834

IJISET - International Journal of Innovative Science, Engineering & Technology, Vol. 6 Issue 5, May 2019
ISSN (Online) 2348 – 7968
www.ijiset.com

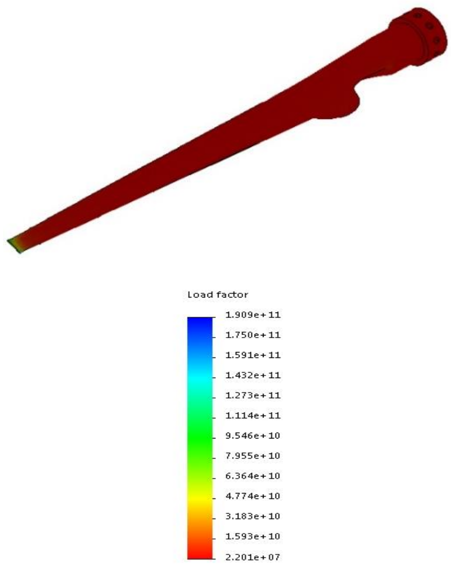

Figure 48: load factor

Dynamic study

Static studies assume that loads are constant or applied very slowly until they reach their full values. Because of this assumption, the velocity and acceleration of each particle of the model is assumed to be zero. As a result, static studies neglect inertial and damping forces.

For many practical cases, loads are not applied slowly or they change with time or frequency. For such cases, a dynamic study is used. Generally if the frequency of a load is larger than 1/3 of the lowest (fundamental) frequency, a dynamic study should be used.

Linear dynamic studies are based on frequency studies. The software calculates the response of the model by accumulating the contribution of each mode to the loading environment. In most cases, only the lower modes contribute significantly to the response. The contribution of a mode depends on the load's frequency content, magnitude, direction, duration, and location.

Objectives of a dynamic analysis include:

- ✓ Design structural and mechanical systems to perform without failure in dynamic environments.
- ✓ *Modify system's characteristics (i.e., geometry, damping mechanisms, material properties, etc.) to reduce vibration effects.*

Name	Type	Min	Max
Stress1	VON: von Mises Stress at Step No: 100(2.4622e-314 Seconds)	3.203e-04 N/mm^2 (MPa) Node: 2629	1.480e+00 N/mm^2 (MPa) Node: 3360

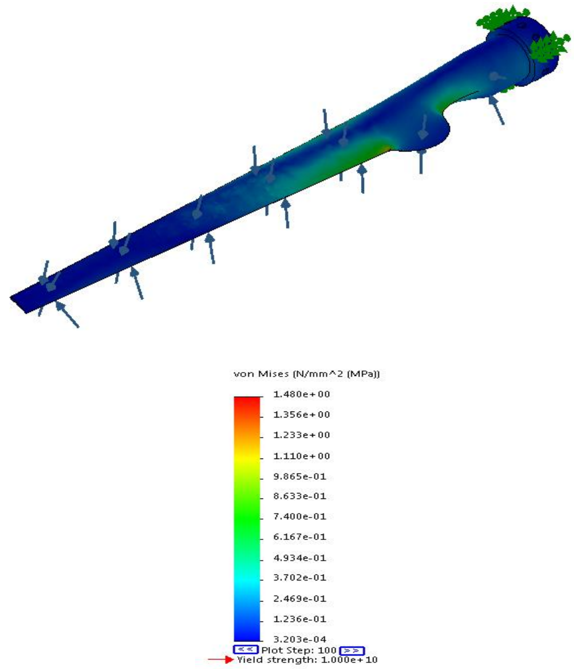

Figure 49: stress analysis

Name	Type	Min	Max
Displacement	URES: Resultant Displacement at Step No: 100(2.4622e-314 Seconds)	0.000e+00 mm Node: 642	1.336e-07 mm Node: 553

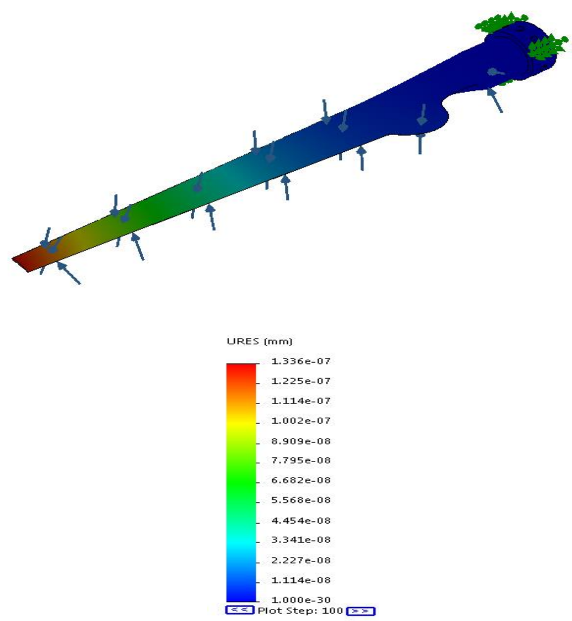

Figure 50: displacement analysis

Name	Type	Min	Max
Velocity1	VRES: Resultant Velocity at Step No: 100(2.4622e-314 Seconds)	0.000e+00 mm/sec Node: 266	2.183e-09 mm/sec Node: 555

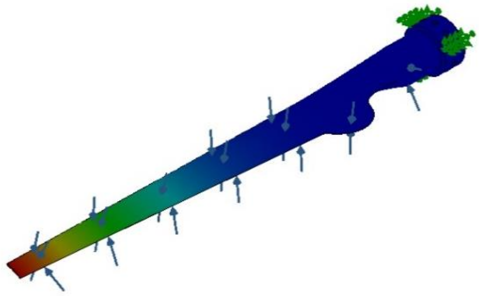

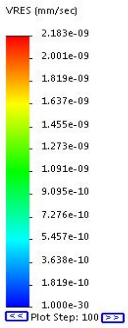

Figure 51: velocity analysis

Dynamic response

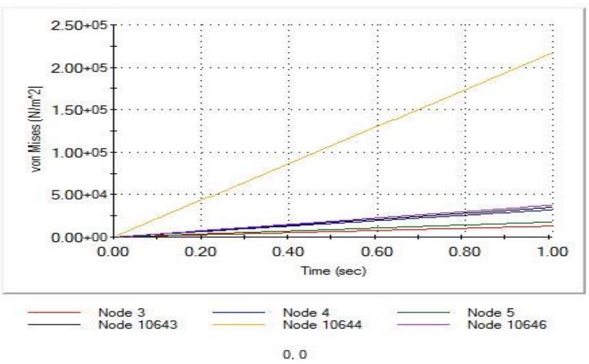

Figure 52: Dynamic response time history graph

Name	Type	Min	Max
Acceleration	ARES: Resultant Acceleration at Step No: 100(2.46221e-314 Seconds)	0.000e+00 mm/s^2 Node: 642	5.320e-03 mm/s^2 Node: 553

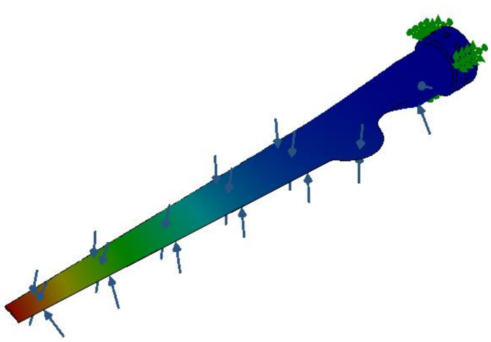

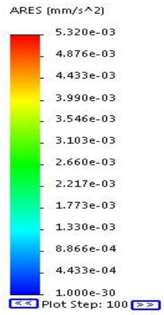

Figure 53: acceleration analysis

Conclusion

This paper presents the analytical, computer aided design of a horizontal axis wind turbine of the rotor blade performance for a 2MW wind turbine for the Ethiopian wind site assessment data of speed and specific area altitude difference consideration based on blade element momentum theory (BEM). The main focus is on the relationship between solidity, pitch angle, tip speed ratio, and maximum power coefficient. In this study, airfoil AH 79-100 C and GOE 239 (MVA H.31) are used but by comparing their performance airfoil GOE 239 (MVA H.31) was selected and studies were conducted, both analytical, computer aided design. This helps to improve the design to get the best wind power extraction airfoil parameters. The computer aided design used in this study are mainly SOLIDWORKS 2019 and MATLAB 2018b which plays a vital role as we see from each analysis.

Based on economics of scale in wind turbines, i.e. larger machines are usually able to deliver electricity at a lower cost than smaller machines. The reason is that the cost of foundations, road building, electrical grid connection, plus a number of components in the turbine (the electronic control system etc.), are somewhat independent of the size of the machine that's why the blade design is focused on large scale (2MW)

Finally with the previous analytical calculation and CAD simulation we can see the difference between currently manufactured blade characterizations with the designed one.

Acknowledgment

I like to express my deepest gratitude and appreciation to my supervisor, Belete Sirahbizu Yigezu (Ph.D) Assistant Professor and University-Industry Linkage Director for his invaluable guidance and encouragement throughout this study and thanks for his patience and trust during the study. Finally I would like to thank my colleagues for their supports.

Nomenclature

a = Axial induction Factor
a' = Tangential induction Factor
A = Area, area swept by turbine blades
B = Number of blades
Cd = Coefficient of Drag
Cl = Coefficient of Lift
CP = Coefficient of Power
c = Chord length
P = Power
r = Radius to annular blade section
T = Torque

$U1$ = Wind Speed Upstream of Rotor U1
$U3$ = Wind Speed Downstream of Rotors
Urel =. Relative Wind Speed
λ = Tip Speed Ratio
α = Angle of Attack
$\varphi = angle\ of\ relative\ wind$
$\theta_P = section\ pitch\ angle$
Γ= Solidity
AEP = Annual energy production
BEM = Blade element momentum
BE = Blade element
nL =The total cycles over a turbine's lifetime
k = number of cyclic events per revolution
n_{rotor}= rotational speed of rotor (rpm),
H_{op}= operating hours per year and
Y = years of operation
σ_g= Maximum stress due to gravity
W= weight of blade
r_{cg} =center of gravity
t = thickness
F_c =stress due to centrifugal force
Udl=uniformly distributed load
V_B shear force
M=moment
A=Structural load on wind turbine
R=Driving force
F_D=drag force
F_L=lift force
F= Prandtl correction factor
p_{blade}= power on blade
η=efficiency
p_w= Power in the air
$vmean$= mean wind speed
$vdesign$=design wind speed

Reference

1) World Wind Energy Association (WWEA), World Wind Energy Report 2016, October 2017.
2) James F. Manwell, Jon G. McGowan, Anthony L. Rogers - Wind energy explained_ theory, design and application (2002, Wiley)
3) IEC_61400_1_1999_EN.pdf
4) Oluleke Oluwole (auth.) - Finite Element Modeling for Materials Engineers Using MATLAB®-Springer-Verlag London (2011)
5) Peter I. Kattan PhD (auth.) - MATLAB Guide to Finite Elements_ An Interactive Approach-Springer-Verlag Berlin Heidelberg (2008)
6) Won_Y._Yang_Wenwu_Cao_Tae-Sang_Chung_John_MorrBookZZ.org_
7) Wind-Power-Turbine-Design-Selection-and-Optimization
8) Barlas, T.; Lackner, M. The Application of Smart Structures for Large Wind Turbine Rotor Blades. In *Proceedings of the Iea Topical Expert Meeting*; Delft University of Technology: Delft, The Netherlands, 2006
9) Ahlstrom, A. Emergency stop simulation using a finite element model developed for large blade deflections. *Wind Energy* 2006
10) Veritas, D.N. *Design and Manufacture of Wind Turbine Blades, Offshore and Onshore Turbines*; Standard DNV-DS-J102; Det Norske Veritas: Copenhagen, Denmark, 2010
11) Chandrala M., Choubey A., Gupta B., 2012. Aerodynamic analysis of horizontal axis wind turbine blade. *Journal of Engineering Research and Application* 2
12) Benini E., Toffolo A., 2005. Optimal design of horizontal-axis wind turbines using blade-element theory and evolutionary computation. *Journal of Solar Energy Engineering*
13) Adama I Wind farm Project Summary Report
14) Case_study-ASHEGODA-WIND-FARM-rev-1
15) EthiopiaWindResourcePosterLandscapeWBESMAPA pr2016_2
16) Ethiopian Electric Power Corporation (EEPCo).Strategic management and programming. Facts in brief; 2011
17) Ethiopian Electric Power Corporation (EEPCo), Strategic plan 2011–2025. Addis Ababa; 2011
18) [IET Energy Engineering 117] Hamid Reza Karimi - Structural Control and Fault Detection of Wind Turbine Systems (2018, The Institution of Engineering and Technology)
19) MATLAB/Simulink SimPowerSystems Documentation. http://www.mathworks.com
20) Turbines, Report number: DCT 2003.90, Eindhoven, 2003.5. P. Rosas, "Dynamic influences of wind power on the power system", Risø -R-1408 (EN), 2003
21) Mulugeta Biadgo Asress et al.: Wind energy resource development in Ethiopia as an alternative energy future beyond the dominant hydropower, Renewable and Sustainable Energy Reviews Vol. 23
22) Eggleston, D.M, and F.S. Stoddard, Wind Turbine Engineering Design, Van Nostrand Reinhold Co. Inc., New York, N.Y., 1987
23) Eurocode 1, Basis of design and actions on structures, Section 2-4: Wind actions on structures
24) David A. Spera, David A. Spera - Wind Turbine Technology_ Fundamental Concepts in Wind Turbine Engineering, Second Edition (2009, ASME Press (American Society of Mechanical Engineers))
25) Gustave Paul Corten - Flow separation on wind turbine blades

Bibliography

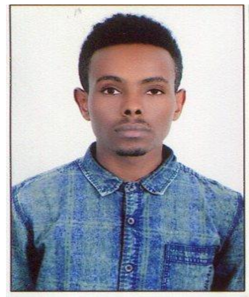

First author

Gizachew Dereje

Lecturer

University of Gondar

Education

2017/18-2019 MSc in Mechanical Engineering (Design) from Addis Ababa science and Technology University

College of mechanical and electrical engineering

Thesis entitled “design and control of 2 MW horizontal axis wind turbine”

2010-2015 BSc in mechanical Engineering from BahirDar institute of technology

Department of mechanical and industrial engineering

Thesis entitled “design of dish washing machine for student’s cafeteria in BahirDar University”

Work experience

December 01/12/2015-September 20/ 2016 in Amhara National Regional State Metal Industry &Machine Technology Development Enterprise in BahirDar City as a Mechanical Design Engineer

September 2016 –onwards in university of Gondar Institute of Technology as lecturer

Research Interest

Research on stress analysis and distribution on a cubic surface by using ANSYS, MATLAB&COMSOL software

Research on fracture mechanics based on central crack using simulation

Research and project on 3D printer

International Conferences and Conference Proceedings

African born 3D printer university of Gondar with collaboration of Kenya

Second author

Belete Sirahbizu Yigezu (Ph.D)

Assistant Professor and University-Industry Linkage Director

Addis Ababa Science and Technology University

EDUCATION

2010 - 2014 Ph.D. in Mechanical Engineering from Indian Institute of Technology Roorkee

Department of Mechanical and Industrial Engineering, Roorkee, Uttarakhand India.

Thesis entitled, “*Some Studies on Wear, Machinability and Weldability of Al-12%Si-TiC In-Situ Composites*”

2006 - 2008 Masters of Science in Mechanical Engineering with specialization in Industrial Engineering from Addis Ababa University Faculty of Technology, Addis Ababa Ethiopia.

Thesis entitled, “*Group Technology for Ethiopian Manufacturing Industries (A Case Study on Hibret Machine Tool Engineering Complex)*”

1998 - 2002 Bachelors of Technology in Mechanical Engineering with specialization in Manufacturing Technology.

Graduate project entitled, “*Development of Tool Path Simulation on Dedicated CAM Software”*

Work Experience

Since 2008 about 6 years I had been working in various industries as a design and manufacturing engineer and since 2008 till date I have been serving in Ethiopian Fedral Higher Education institutions as instructor, researcher and various administrative position.

Research Interest

✓ Modeling and Experimental Analysis of Metal Matrix Composite and Ceramic Composite Materials

- ✓ Design and Analysis of Renewable Energy Sources.
- ✓ Design and Experimental Analysis of Shape Memory Polymer based Composite Materials
- ✓ Design, Modeling and Optimization of Fusion and Solid State Joining parameters of Steel and Metal Matrix Composite Structures

List of Selected Publications

Belete Sirahbizu Yigezu, P. K. Jha & M. M. Mahapatra. Influence of reinforcement type on microstructure, hardness, and tensile properties of an aluminum alloy metal matrix composite**,** *Journal of Minerals and Materials Characterization and Engineering*, 2013, 1, 124-130.

Belete Sirahbizu Yigezu, P. K. Jha & M. M. Mahapatra, “The as cast microstructure and mechanical properties of 10wt%TiC reinforced Al-12%Si matrix composite” *American Journal of Materials Science and Application*, 2014, 2(4), 50-55.

Belete Sirahbizu Yigezu, P. K. Jha & M. M. Mahapatra. Effect of sliding distance, applied load, and weight percentage of reinforcement on the abrasive wear properties of in situ synthesized Al–12%Si/TiC composites, Tribology Transactions, 2013, 56, 546-554.

Belete Sirahbizu Yigezu, P. K. Jha & M. M. Mahapatra, “Effects of In-situ TiC Reinforcements on the Machining Process Characteristics of Al+12Si Matrix”, *American Journal of Materials Science and Application*, 2014, 2(4), 56-62.

Belete Sirahbizu Yigezu, M. M. Mahapatra, P.K. Jha. The key attributes of synthesizing ceramic particulate reinforced Al based matrix composites through stir casting process, a review, *Materials and Manufacturing Processes*, 2013, 28, 969–979.4

Belete Sirahbizu Yigezu, D. Venkateswarlu, M. M. Mahapatra, P. K. Jha & N. R. Mandal. On friction stir butt welding of Al+12Si/10wt%TiC *in-situ* composite, *Materials and Design*, 2014, 54, 1019–1027.

Belete Sirahbizu Yigezu, M.M. Mahapatra & P.K. Jha. On modeling the abrasive wear characteristics of in situ Al–12%Si/TiC composites, *Materials and Design*, 2013, 50, 277– 284.

International Conferences and Conference Proceedings

- ✓ **Belete S. Y.**, Mahapatra. M. M. and Jha P. K. Mechanical property and abrasive wear characteristics of in-situ synthesized Al+12Si/10TiC composites. TMS 2013 **Supplemental Proceedings,** Part XX: Recent Developments in the Processing, Characterization, Properties, Performance and Applications of Metal Matrix Composites, 2013, 1053-1060.
- ✓ **Belete S. Y.**, Kumar A., Jha P. K. and Mahapatra M. M. A comparative study on the properties and microstructure of Al-12%Si and Al-4.5%Cu alloys reinforced with 5wt% TiC, International Conference on Advances in Materials and Processing: Challenges and Opportunities (AMCO 2012), November 2-4, **2012**, IIT Roorkee, India.
- ✓ **Belete S. Y.**, Mahapatra. M. M. and Jha P. K. Investigation on machinability characteristics of synthesized Al+12Si/10wt.%TiC in-situ composites. 2nd International Conference and Exhibition on Materials Science and Engineering, October 07- 09, **2013**, Hampton Inn Tropicana, Las Vegas, NV, USA.
- ✓ Birru A. K., **Belete S. Y.**, Chinatala V., Mahapatra M. M., Karunakar D.B. and Kumar P. Influence of pouring temperature and mould coating on fluidity in A40E and A713 aluminum alloys, Procedings of the 5th International Conference on Advances in Mechanical Engineering (ICAME-2011), June 06-08, 2011 S.V. National Institute of Technology, Gujarat, India, **2011,** 815-818.